An Integrated CFD and Experimental Analysis on Double-Skin Window

Sheam-Chyun Lin, Wei-Kai Chen, Hung-Cheng Yen, Yung-Jen Cheng, Yu-Cheng Chen

Abstract—Result from the constant dwindle in natural resources, the alternative way to reduce the costs in our daily life would be urgent to be found in the near future. As the ancient technique based on the theory of solar chimney since roman times, the double-skin façade are simply composed of two large glass panels in purpose of daylighting and also natural ventilation in the daytime. Double-skin façade is generally installed on the exterior side of buildings as function as the window, so there is always a huge amount of passive solar energy the façade would receive to induce the airflow every sunny day. Therefore, this article imposes a domestic double-skin window for residential usage and attempts to improve the volume flow rate inside the cavity between the panels by the frame geometry design, the installation of outlet guide plate and the solar energy collection system. Note that the numerical analyses are applied to investigate the characteristics of flow field, and the boundary conditions in the simulation are totally based on the practical experiment of the original prototype. Then we redesign the prototype from the knowledge of the numerical results and fluid dynamic theory, and later the experiments of modified prototype will be conducted to verify the simulation results. The velocities at the inlet of each case are increase by 5%, 45% and 15% from the experimental data, and also the numerical simulation results reported 20% improvement in volume flow rate both for the frame geometry design and installation of outlet guide plate.

Keywords—Solar energy, Double-skin façades, Thermal buoyancy, Fluid machinery.

I. INTRODUCTION

PUSHING air with rotating impeller derived by motors is the most common way to generate air movement after the Industrial Revolution. The practical devices such as mechanical fan, pump, and compressor require considerable electric power supply and furthermore make noises during high-speed operation. Many scientists have been researching on this mechanism so called force convection ever since the mechanical fans are practically applied in diverse cooling systems. Nowadays the force convections are widely used to solve engineering problems; however the natural convection which is another neglected convective mechanism occurs very frequently in our everyday life.

The flow movement of natural convection is induced by an

S. C. Lin, W. K. Chen, and Yu-Cheng Chen are with the Department of Mechanical Engineering, National Taiwan University of Science and Technology, Taipei, Taiwan 10672 (phone: 02-2737-6453; fax: 02-2737-6460; e-mail: sclynn@mail.ntust.edu.tw and m9903302@mail.ntust.edu.tw).

H. C. Yen is with Industrial Technology Research Institute and Department of Mechanical Engineering, National Chiao Tung University, Hsinchu, Taiwan 300 (e-mail: BRIANYEN@itri.org.tw).

Y. J. Cheng is with Industrial Technology Research Institute, Hsinchu, Taiwan 300 (e-mail: eric_cheng@itri.org.tw).
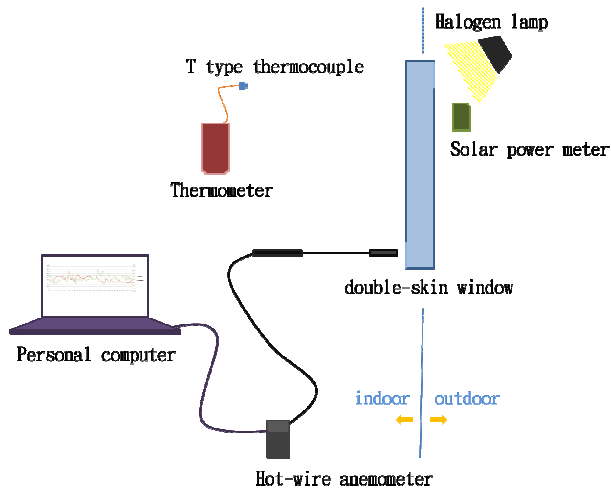
internal force, and this mechanism is strongly related to the temperature gradient. The air expands and becomes less dense when the temperature rises, so the air with lower density will be pushed upward by the buoyance resulting from the gravity. This convection phenomenon exists commonly during summertime when the air molecules are much more dynamic than in winter.

The convectional rain would be a good example to explain why there is more precipitation in summer. The moisture is a small amount of water in the air, and the air would go upward to the sky when heated by the solar radiation. The accumulated of water droplets, frozen water crystal, and some other chemicals in the sky will become cloud layers. As the buoyant force of upward convectional airflow can no more balance with the weight of the cloud, the water drop in the cloud would fall down to the ground surface, the so called convectional rainfall. Then after the rainfall, the water on the ground absorbs the heat from the surrounding to evaporates, so the environmental temperature will decrease, and at the mean time the natural convection decrease. Therefore, the sky is normally clear and blue on a summer night.

Natural convection is really closed to our daily life but was infrequently utilized to solve engineering problems. Hence, this study imposes a double-skin window to generate airflow for the indoor ventilation. The structure is simply composed of two layers of glass panel, and the air in the cavity absorbs the heat energy when the solar radiation passes through the window [1]-[3]. Then the air with higher temperature would rise because of the density gradient. The replenishment of the air at the bottom part of the window come from the indoor where the temperature is lower compare to the cavity, so the density at the bottom would be always lower to induce the airflow inside the cavity due to the convective phenomena. Several previous researches on the double-skin window are executed worldwide to seek the possibility in applying the ventilation via natural convection [4]-[6]; however, it is essential to evaluate this device based on the local environment information for any realistic application. Thus, this study primarily discusses the application of natural convection instead of force convection, and how to increase the volume flow rate of the domestic double-skin window would be the main objective in this topic.

II. EXPERIMENTAL APPARATUS

The research instruments include double-skin window, hot-wire anemometer, thermometer, solar power meter, T type thermocouple, halogen lamp and personal computer. The personal computer was set to record the real time data from the anemometer, and the entire system was shown in Fig. 1.

Fig. 1 The experimental apparatus system

Fig. 2 The floor plan of the test site

Fig. 3 The dimension of original prototype

Fig. 4 The hot-wire anemometer

The indoor, outdoor temperature and temperature difference between both are all the important factors to the performance of double-skin window, so the above parameters would be measured at beginning of the test. To avoid the wind disturb the pressure at the boundary, we chose a classroom close to a corridor by the side of the building exterior walls. The double-skin window is installed on the wall between the classroom and the corridor, and because there are several windows between the corridor and the exterior, we closed the windows to avoid the wind blowing into the corridor to influence test.

Indoor air would be pushed outward due to the thermal expansion when the temperature is higher than the outdoor, and the flow direction would be opposite when outdoor temperature is higher on the same principle. Therefore, a small clearance between windows is left in classroom and corridor sides to balance the pressure generated from the above phenomenon for ensuring the equivalent pressures at the upstream and downstream conditions. Also, the curtain is utilized to cover those gaps for eliminating the possibility of perturbed wind from outsides. The floor plan of the test site is shown in Fig. 2.

The dimension of the original prototype refers to the general size of residential windows, and the cavity thickness was designed as the minimum size (> 20 cm) as load-bearing wall of common building in Taiwan. According the above references we design the first prototype of double-skin window with 1m in length, 0.5m in width, 0.2m in thickness of cavity and two 0.15m × 0.5m airflow outlets at the top and bottom side. The test model made by 0.05m thick acrylic boards is shown in Fig. 3.

A 500W halogen lamp is used in the experiment to simulate the solar radiation, and the amount of 1423W/m2 which is the maximum solar radiation on the earth surface can be measure 7-8cm from the halogen lamp in the practical test. We put the lamp 1m away face to the double-skin window and apply the same boundary condition later in the numerical analysis.
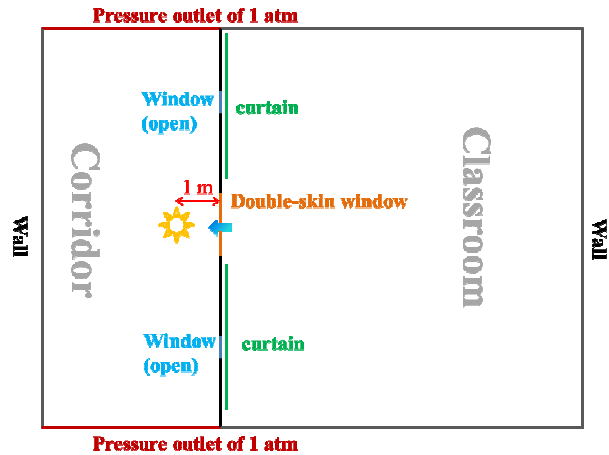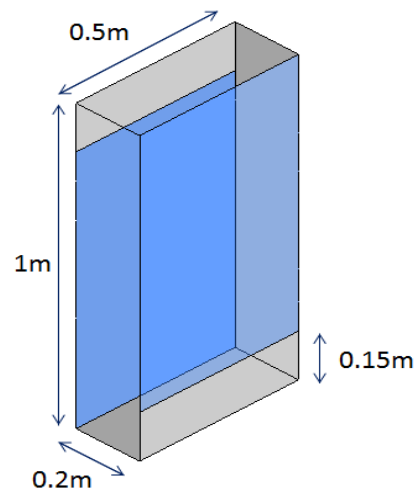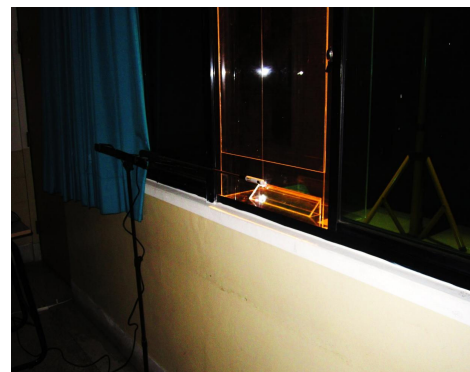
Solar elevation angle is about 60 to 80 degrees in summer in Taiwan, so the elevation of the halogen lamp was set at 70 degrees in the experiment. The purpose of the study is to improve the efficiency of double-skin window for ventilation. The measurement will be focused on the inlet which is the interface connect to the indoor to see how much air the

double-skin window can take from the classroom. The hot-wire anemometer (shown in Fig. 4) was set to record the real time data of airflow temperature and velocity, and the smoke was also applied to check the airflow direction.

III. NUMERICAL SCHEME

To simulate the induced flow inside the cavity of double-skin window, the commercial CFD software Fluent [7] is utilized to solve the fully three-dimensional incompressible Navier- Stokes equations with the standard turbulence model, and the LES turbulence model is adopted to calculate the oscillation of velocity and temperature result from the thermal effect. The following subsections describe the mathematical models, boundary conditions, and grid verification used in the numerical approach.

A. Governing Equation and Turbulent Model

The continuity and momentum equations in conservation form are expressed as:

Continuity equation

$$\frac{\partial u_i}{\partial x_i} = S_m \tag{1}$$

where u_i and S_m are the velocity tensor and the source term, respectively.

Momentum equation

$$\rho \frac{\partial u_i}{\partial t} + \rho \frac{\partial (u_i u_j)}{\partial x_j} = -\frac{\partial p}{\partial x_i} + \frac{\partial}{\partial x_j}\left(\mu\left(\frac{\partial u_i}{\partial x_j} + \frac{\partial u_j}{\partial x_i}\right)\right) + \rho g_i + F_i \tag{2}$$

where g_i is the gravity, and F_i is the body force.

When the fluid inertia affects the flow field more significantly than the fluid viscosity, the flow develops into a turbulent flow. Turbulent flows are characterized by fluctuating velocity fields, and cause many eddies due to this fluctuation. This study utilizes the $k - \varepsilon$ turbulence model to solve the Navier-Stokes equations.

$$\frac{\partial}{\partial t}(\rho u_i) + \frac{\partial}{\partial x_j}(\rho u_i u_j) = -\frac{\partial p}{\partial x_i} + \frac{\partial}{\partial x_j}\left[\mu\left(\frac{\partial u_i}{\partial x_j} + \frac{\partial u_j}{\partial x_i} - \frac{2}{3}\delta_{ij}\frac{\partial u_l}{\partial x_l}\right)\right] \tag{3}$$
$$+ \frac{\partial}{\partial x_j}\left(-\rho\overline{u_i' u_j'}\right)$$

where the Reynolds stresses are modeled employing the Boussinesq hypothesis [8]. In addition, the turbulent viscosity μ_t is computed as a function of turbulence kinetic energy (k) and turbulence dissipation rate (ε):

$$-\rho\overline{u_i' u_j'} = \mu_t\left(\frac{\partial u_i}{\partial x_j} + \frac{\partial u_j}{\partial x_i}\right) - \frac{2}{3}\left(\rho k + \mu_t \frac{\partial u_i}{\partial x_i}\right)\delta_{ij} \tag{4}$$

$$\frac{\partial}{\partial t}(\rho k) + \frac{\partial}{\partial x_i}(\rho k \mu_i) = \frac{\partial}{\partial x_j}\left[\left(\mu + \frac{\mu_t}{\sigma_k}\right)\frac{\partial k}{\partial x_j}\right] \tag{5}$$
$$+ G_k + G_b - \rho\varepsilon - Y_M + S_k$$

$$\frac{\partial}{\partial t}(\rho \varepsilon) + \frac{\partial}{\partial x_i}(\rho \varepsilon \mu_i) = \frac{\partial}{\partial x_j}\left[\left(\mu + \frac{\mu_t}{\sigma_\varepsilon}\right)\frac{\partial \varepsilon}{\partial x_j}\right] + G_{1\varepsilon}\frac{\varepsilon}{k}(G_k + C_{3\varepsilon}G_b) \tag{6}$$
$$- C_{2\varepsilon}\rho\frac{\varepsilon^2}{k} + S_\varepsilon$$

$$\mu_t = \rho C_\mu \frac{\kappa^2}{\varepsilon} \tag{7}$$

where G_k and G_b are the turbulent kinetic energy generated by the mean velocity gradients and buoyancy, respectively. Y_M represents the contribution of the fluctuating dilatation in compressible turbulence to the overall dissipation rate, and C_μ, $C_{1\varepsilon}$, $C_{2\varepsilon}$, $C_{3\varepsilon}$, σ_k and σ_ε are model constants [9].

In addition to the $k - \varepsilon$ model, this study adopts the LES turbulence model to solve the large eddies in this unsteady flow field for the purpose of calculating sound pressure. The LES model solves large eddies directly by filtering the time-dependent Navier-Stokes equations, while small eddies are computed using the subgrid-scale Smagorinsky-Lilly model. A filtered variable is defined by

$$\overline{\phi}(x) = \int_D \phi(x')\ G(x, x')\ dx' \tag{8}$$

where D is the fluid domain, and G is the filter function that determines the scale of the resolved eddies. Through finite-volume discretization, the filtering operation can be represented as

$$\overline{\phi}(x) = \frac{1}{V}\int_\upsilon \phi(x')\ dx',\ \ x' \in \upsilon \tag{9}$$

where V is the volume of a computational cell. The filter function $G(x, x')$ determines the filter scale and executes the filter process

$$G(x, x') = \begin{cases} \dfrac{1}{V}, x' \in \upsilon \\ 0, x' \notin \upsilon \end{cases} \tag{10}$$

Filtering the Navier-Stokes equation leads to

$$\frac{\partial \overline{u}_i}{\partial x_i} = 0 \tag{11}$$

$$\rho \frac{\partial \overline{u}_i}{\partial t} + \rho \frac{\partial (\overline{u}_i \overline{u}_j)}{\partial x_j} = \frac{\partial}{\partial x_j}\left(\mu \frac{\partial \sigma_{ij}}{\partial x_j}\right) - \frac{\partial \overline{p}}{\partial x_i} - \frac{\partial \tau_{ij}}{\partial x_j} \tag{12}$$

where σ_{ij} and τ_{ij} are the stress tensors due to molecular viscosity and the subgrid-scale stress, respectively.

B. Boundary Conditions

In this work, several appropriate assumptions and boundary conditions were made to simulate the actual flow patterns inside the double-skin window. They are described as follows:

(1) Pressure Outlet Boundary Condition

We measure the actual indoor and outdoor ambient temperature and apply the data to the pressure outlet boundary at the upstream and downstream of the double-skin window. The pressure at outlet surface is set to be one atmosphere.

(2) Wall Boundary Condition

This numerical model sets the no-slip boundary condition on the solid surfaces of the wall.

(3) Radiation Energy Input

The ray tracing method is applied to simulate the sun rays. The energy rays will be set as a source term in the energy equation, and enter the numerical model from the outdoor atmospheric boundary. The energy transportation inside the model would be calculated based on the penetration rate of transmissivity and reflectivity.

(4) Window Wall Optical Conditions

The optical conditions on the surface of the double-skin window are applied to simulate the transparent material. Generally, lights would be divided into three ways which are reflection, absorption and penetration when passing through a transparent interface between the air and the glass, and furthermore the reflection includes specular and diffuse reflection. Therefore, the absorptivity and transmissivity of the transparent material should be applied in the numerical simulation of the research.

(5) The Boundary Condition Setting

In addition to the conditions discussed above, to simplify the calculation the study would take following assumptions:
a. Newtonian fluid is applied as the air density would be calculated from the Boussinesq approximation.
b. Thermal conductivity (k), viscosity coefficient (μ) and specific heat (Cp) are independent from the pressure.
c. Consider thermal buoyancy effects, so do the effect of gravity.

IV. EXPERIMENTAL AND SIMULATION RESULTS

The internal force inducing the natural convection is quite weak compare to the force convection. Therefore, the considerable experimental error might occur since the control volume is not easy to build for a double-skin window because of the possibility of pressure resistance. The wind and any objective on the airway could disturb the test result. However, the trends of velocity in the test results and the trends of volume flow rate in the simulation result both offer us a diagrammatic flow pattern to investigate, so experiments and simulations are actually useful to modify the case.

The study at this section is separated into three branches which are the frame geometry design, the installation of outlet guide plate and the solar energy collection system to discuss each improvement independently. They are described as follows:

A. Frame Geometry Design

In the original design, there are two large vortexes at the center and the bottom parts in the cavity. When airflow is brought into the cavity at the bottom, first it hits the vertical surface of the outer glass and separate into up and down flow. The down flow will hit the bottom surface result in the bottom vortex, and the up flow will be draw by the internal force of the natural convection at the center and accelerated upward to the top. The vortex at the center results from the asymmetric flow pattern. The main stream in the cavity goes along the surface of outer glass, so the vertex is generated at the reign beside another surface due to the flow friction. Therefore, we design a wedge strip at the entrance and reduce the length of inner window to form a chamfer at the top. The wedge stripe can guide the inlet flow along the vertical direction and when the flow reaches the top, the chamfer will guide the flow leave the cavity. The modified design is shown in the Fig. 5. A numerical visualization on a forward section is shown in Fig. 6, and the test and numerical data are listed in Table I.

TABLE I
RESULT OF THE FRAME GEOMETRY DESIGN AND THE ORIGINAL PROTOTYPE

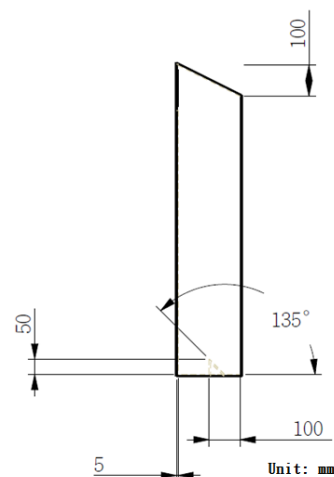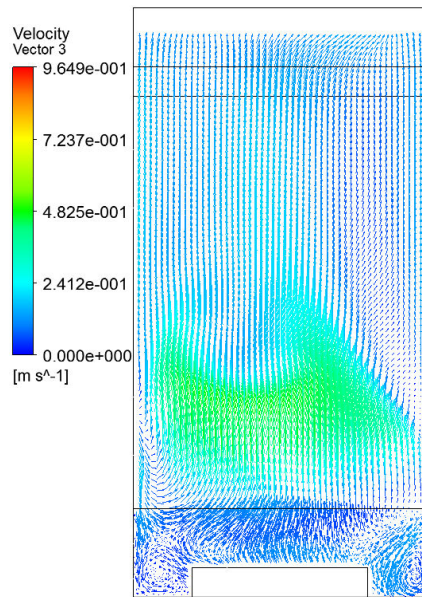|		Frame design	Original	Improved ratio
Experimental data		0.39 m/s	0.36 m/s	8%
Numerical result	V	0.45 m/s	0.427 m/s	5%
	Q	30 cfm	24.8 cfm	20%
Environmental conditions				
Indoor temperature : 22.5℃				
Outdoor temperature : 21.5℃				
Solar radiation input : 1,423 W/ m²				
Solar zenith angle : 70°				

Fig. 5 Frame geometry design

Fig. 6 (a) Calculated velocity distributions at the front section for the frame geometry design
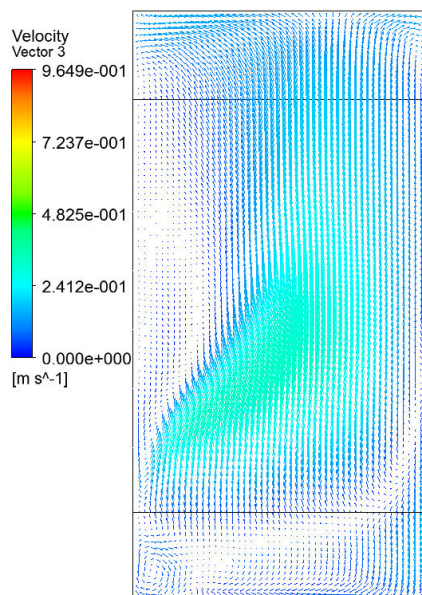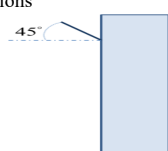

Fig. 6 (b) Calculated velocity distributions at the front section for the original prototype

B. Outlet Guide Plate

The outlet guide plate can not only extend the airway of the induced flow but also be an exterior shade to prevent the wind. This design smoothens the stream line at cavity outlet and improves the air velocity practically, so do the volume flow rate. From the numerical visualization as shown in Fig. 7, we can see the fluid field changes after the installation of the guide plate. A plastic plate with 15cm in length is set 45° to the horizontal at the outlet of the cavity in the test. The results of the simulation and the experiment are both listed in Table II.

TABLE II
RESULT OF THE OUTLET GUIDE PLATE DESIGN AND THE ORIGINAL PROTOTYPE

		Guide plate	Original	Improved ratio
Experimental data	30°	0.13 m/s		18%
	45°	0.16 m/s	0.11 m/s	45%
	60°	0.07 m/s		-30%
	70°	0.12 m/s		9%
Numerical result	V	0.168 m/s	0.157 m/s	7%
	Q	20.7 cfm	17.3 cfm	19.6%
Environmental conditions				

Indoor temperature：21.5℃

Outdoor temperature：21℃

Solar radiation input：1,423W/ m^2
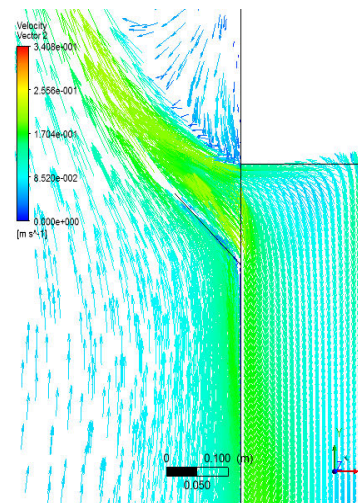
Solar zenith angle：70°

Fig. 7 (a) Calculated velocity distributions at the outlet section for the frame geometry design
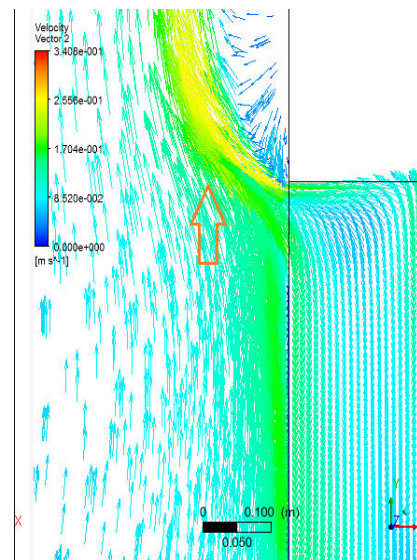

Fig. 7 (b) Calculated velocity distributions at the outlet section for the original prototype

C. Solar Collection System

Solar radiation offers the main power source to the double-skin window. To improve the absorption of solar energy, we design a solar collection system composed of one concave mirror and one aluminum rod, and the focus phenomenon is shown in Fig. 8. The system is set at the bottom so it will not reduce the function of daylighting. Once the sunlight enter the cavity, the minor would reflect the light to the focus on which the rod is set, so the air inside the cavity can receive more heat to produce air movement. The test result is shown in Table III.

TABLE III
RESULT OF THE SOLAR COLLECTION SYSTEM DESIGN AND THE ORIGINAL PROTOTYPE

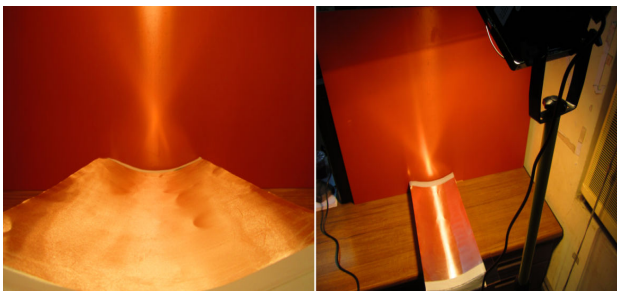| Experimental data	Solar collection 0.32 m/s	Original 0.278 m/s	Improved ratio 15%
	Environmental conditions		
	Indoor temperature：21.5℃		
	Outdoor temperature：18.5℃		
	Solar radiation input：1,423W/ m^2		
	Solar zenith angle：70°		

Fig. 8 Optical focus phenomenon

V. THERMAL BUOYANCE EFFECT

The mechanism of the convective heat transfer always includes the fluid movement which is the main topic in the research, and generally the induced airflow goes upward opposite to the direction of gravity by the internal force generate from the density difference. The density difference is result from the temperature gradient cause by the heat input to the flow field, so when the warmer air is push upward due to the expansion, the cooler air will be draw into the upstream of the airflow, and therefore the temperature in the field would decrease until the external energy input heat the air again.

We observe the phenomena described above in the test. As the result shown in Fig. 9, we can see the periodic oscillations of the temperature and the velocity, and even later in the numerical analysis, we get the same result with the transient large eddy simulation of the flow field in the double-skin window.
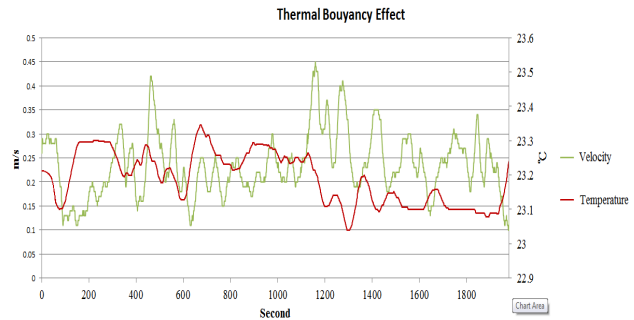

Fig. 9 The periodic oscillations of temperature and velocity in the cavity

VI. RESULTS AND DISCUSSIONS

In this study, an integrated performance analysis for a double-skin window is carried out through a combined experimental and numerical approach, and several tests were conducted for each case in different environments. We have found that when the overall environmental temperature is higher, the effect of thermal convection would be stronger to contribute to the volume flow rate of the double-skin window, and also if the indoor temperature surpasses outdoor temperature more, the phenomena would become more obvious.

The frame geometry design, the outlet guide plate and the solar collection system offer severally 5%, 45% and 15% velocity improvement compare to the original design in the practical test. We can see the flow field become much smoother from the numerical visualization for the first case, and the vortex at the bottom also shrink due to the wedge stipe.

In the second case, the velocity improves largely in the practical test. However, from the numerical result, the improvement is not so huge. The velocity only raises 7% in the numerical analysis. That is because in the practical test, we cannot perfectly prevent the wind from influencing the experimental apparatus. While the main function of the guild plate is to get rid of the wind pressure, so in the windless condition of numerical analysis, the performance of guide plate is not so obvious.

The flow velocity should be proportional to the volume flow rate when pass through a same area, and as we can see the result is in accordance with the theory. The volume flow rates are enhanced 20% both in the first two cases.

The application of double-skin window might be limited to three-story buildings or below. The wind noise occurs quite possibly on the exterior wall of skyscrapers because of the urban canyon effect, so the stacked double-skin façade system bringing the flow to the roof might be a good solution in the situation.

Although the double-skin system cannot function without sunlight, it still opens a possible duct for another mode of ventilation and reduces the outdoor noise due to two layers of isolation.

REFERENCES

[1] Elisabeth Gratia, André De Herde, "Natural ventilation in a double-skin façade," *Energy and Buildings*, vol.36, Feb. 2004, pp. 137-146.

[2] Neveen Hamza, Chris Underwood. "CFD supported modeling of double skin façade in hot arid climates," Ninth International IBPSA Conference, Montréal, Canada, Aug. 2005, pp. 365-372.

[3] H. Manz, Th. Frank. "Thermal simulation of Building with double-skin facades," *Energy and Buildings*, vol.37, Nov. 2005, pp. 1114-1121.

[4] W. Ding, Y. Hasemi, T. Yamada. "Natural ventilation performance of a double-skin façade with a solar chimney," *Energy and Buildings*, vol.37, Apr. 2005, pp. 411-418.

[5] Nassim Safer, Monika Woloszyn, Jean-Jacques Roux, Gilles Rusaouën and Frederic Kuznik. "Modeling of the double-skin façade for building energy simulation radiations: radiative and convective heat transfer," Ninth International IBPSA Conference, Montréal, Canada, Aug. 2005, pp. 1067-1074.

[6] Chun-Hsiung Wang. "Numerical. Simulation of Passenger thermal Comfort inside a Car Cabin," Taiwan University of Science and Technology, Master's dissertation, 2006.

[7] Fluent 6.2 documentation. Fluent Inc.; 2004.

[8] Hinze JO. Turbulence. McGraw-Hill Publishing Co., New York; 1975.

[9] Launder BE, Spalding DB. Lectures in mathematical models of turbulence. Academic Press, London, England; 1972.